

1 **Working title:** Discharge and suspended sediment time series as controls on fine
2 sediment ingress into gravel river beds

3
4

5 Kate L. Mathers^{1*}, Stephen P. Rice² and Paul J. Wood²

6

7 1. Eawag, Department of Surface Waters Research and Management,
8 6047 Kastanienbaum, Switzerland

9 2. Geography and Environment, Centre for Hydrological and Ecosystem Science,
10 Loughborough University, Loughborough, UK

11 **Author for Correspondence**

12 Kate Mathers

13 Eawag,

14 Department of Surface Waters Research and Management,

15 6047 Kastanienbaum, Switzerland

16 Email:- kate.mathers@eawag.ch

17

18

19

20

21

22

23

24

25

26

27

28

29

30

31

32

33

34

35

36 **Working title: Discharge and suspended sediment time series as controls on**
37 **fine sediment ingress into gravel river beds**

38

39 **Mathers, K.L, Rice, S.P. and Wood, P.J.**

40

41 **Abstract**

42 Fine sediment availability and channel hydraulics are two of the primary controls on
43 the ingress of fine sediment into gravel river beds. A novel dataset consisting of fine
44 sediment ingress measurements coupled with high-resolution turbidity and discharge
45 time series, was analysed to investigate relations between ingress, discharge and
46 turbidity. Discharge and turbidity demonstrated a weak association with each other,
47 and their relations with fine sediment ingress were relatively weak. An alternative,
48 but widely applied 'redundancy' approach was investigated that focused on key
49 metrics, or facets, of the discharge and turbidity time series and their association
50 with fine sediment ingress. Principal component analysis was used to distil the most
51 important facets driving variation in the discharge and turbidity datasets and these
52 were then used as independent variables in regression models with sediment
53 ingress as the dependent variable. These models accounted for a larger amount of
54 the statistical variation in sediment ingress over time than discharge and turbidity
55 time series. Facets of the turbidity time series were found to be the most effective
56 explanatory variables. The results suggest that this approach could be valuable and
57 justify its application and testing across a range of river types in different hydrological
58 and sedimentary settings. Application of this method could improve our generic
59 understanding of what controls ingress at larger spatial and temporal scales and
60 therefore complements process-based approaches, which is vital for the
61 development of fine sediment management strategies.

62

63 **Keywords:** sedimentation, redundancy approach, principal component analysis,
64 facets, management.

65

66

67

68

69

70 **1. Introduction**

71 Excessive sedimentation within aquatic ecosystems is a global concern and can
72 have detrimental consequences for all aspects of lotic ecosystem health (Heppell et
73 al., 2009; Relyea et al., 2012; Naden et al., 2016). The deleterious effects of fine
74 sediment on biota are well documented and are predominantly associated with
75 sediment deposition onto, and ingress into, the river bed (Kemp et al., 2011; Jones
76 et al., 2012a, b; 2014). Effective management of fine sediment loading therefore
77 requires understanding of the relations between deposition and ingress and their key
78 drivers, including sediment supply and water discharge (Diplas and Parker, 1992) at
79 scales that are relevant to catchment management.

80 Fine sediment deposition into a framework of gravel clasts involves a complex set of
81 processes. Ingress rates are related to several factors including local hydraulics
82 (Buffington and Montgomery, 1999), vertical and lateral interstitial exchange
83 (Mathers and Wood, 2016), the relative size of the infiltrating and framework
84 particles (Gibson et al., 2009), the concentration of suspended sediment and the
85 settling flux (Brunke, 1999), and sediment transport capacity (Naden et al., 2016).
86 Local hydraulic characteristics such as shear stress, flow velocity and Froude
87 number have been associated with fine sediment accumulation, but studies often
88 disagree regarding the gross influence of these hydraulic parameters (Petticrew et
89 al., 2007). Beschta and Jackson (1979) found that the Froude number was positively
90 associated with ingress, whilst Einstein (1968) and Carling (1984) found no
91 relationship with flow parameters. It is possible that local hydraulic influences differ
92 as a function of the dominant hydrological process. In low energy, slow-flowing
93 waters, fine sediment ingress rates can be high because deposition rates are
94 enhanced (Wood and Armitage, 1999), whereas in high-velocity areas sediment
95 supply can be accentuated, enhancing the availability of fine sediment for
96 subsequent infiltration (Frostick et al., 1984). As such, the availability of fines, as
97 regulated by supply, transport capacity and, potentially biotic effects (e.g. Rice et al.,
98 2016) may dominate the rate of infiltration irrespective of local hydraulics and
99 framework size (Carling and McCahon, 1987; Sear, 1993).

100 Despite an enhanced understanding of the small-scale processes that control fine
101 sediment infiltration (grains to patches; seconds to minutes) there is still no simple

102 predictive model of fine sediment ingress than can be applied at large spatial and
103 temporal scales. Moreover, despite a general understanding that both local
104 hydraulics and sediment supply respond to hydrological processes that occur over
105 longer, monthly-annual timescales, few studies have investigated the relations, over
106 longer timescales, between variations in fine sediment ingress, suspended sediment
107 concentrations and river discharge. This is unfortunate because there is a global
108 need to set river management targets that maintain healthy rates of fine sediment
109 delivery, deposition and transport (Collins et al., 2011) and gaining an understanding
110 of the factors that influence fine sediment ingress on such time-scales is vital for
111 developing relevant management strategies (e.g. Naden et al., 2016).

112 Both field and laboratory studies have identified fine sediment availability as a key
113 determinant of ingress rates (Petts, 1984; Sear, 1993), with positive associations
114 between suspended sediment concentration and ingress (Beschta and Jackson,
115 1979; Carling, 1984; Carling and McCahon, 1987). In general, fine sediment ingress
116 rates are greatest during flood events when sediment transport rates are high and
117 sediment is made available by scouring from pools and sub-armour deposits or is
118 recruited to the channel via overland flow and other processes, including river bank
119 collapse (Beschta et al., 1981; Sear, 1993; Petticrew et al., 2007). However, there is
120 an apparent absence of studies which simultaneously investigate the relationship
121 between flow, sediment supply and deposition to assess the potential explanatory
122 power of different facets of these regimes (Wohl et al., 2015). Direct data on
123 sediment transport and subsequent deposition is severely limited relative to river
124 discharge and there is a need for more high resolution and long term suspended
125 sediment data in order to characterise the magnitude, frequency, duration, timing
126 and rate of change in suspended sediment levels (*sensu* Richter et al., 1996; Poff et
127 al., 1997). Seeking greater understanding of the relations between the drivers and
128 rates of fine sediment ingress over monthly-annual timescales is therefore valuable
129 and consistent with Wohl et al.'s (2015) argument that the fine sediment regime can
130 be managed through consideration of gross water and sediment balances.

131 In this regard, it is possible that ecohydrological approaches, which utilise a
132 redundancy' methodology to associate key elements of hydrological time series with
133 measurements of ecological health, may be useful (Richter et al., 1996; Olden and

134 Poff, 2003). The purpose of such research has been to determine the ecologically
135 relevant components or 'facets' of discharge time series (duration, timing, frequency,
136 magnitude, rate of change in flow events; Richter et al., 1996; 1997; Poff et al., 1997)
137 that support ecologically healthy rivers, thereby facilitating the design of
138 'environmental flows' (Acreman and Ferguson, 2009; Wharfe et al., 2014; Mustonen
139 et al., 2016). Natural variability in stream processes is vital in maintaining diverse
140 and healthy systems (Arthington et al., 2006) and these facets, rather than single
141 simplistic metrics of a dynamic time series, are more appropriate for setting
142 management targets (Richter et al., 1997). Given the plethora of indices that can be
143 obtained from time series data (Poff, 1996), researchers must select which and how
144 many indices are relevant to use for modelling purposes, particularly when many are
145 inter-correlated (Olden and Poff, 2003).

146

147 Principal component analysis, a well-established multivariate technique, enables
148 several variables that are inter-correlated to be analysed for the degree of similarity
149 they characterise and subsequently transformed into a number of uncorrelated axes
150 (variables) called 'principal components' which represent linear combinations of the
151 original variables (Abdi and Williams, 2010). By identifying a reduced set of indices
152 that represent the degree of variability in the time series, annual river management
153 targets can be identified using a comprehensive statistical characterisation of
154 relevant regime characteristics (Richter et al., 1997). This is an explicitly empirical
155 method that requires careful application to avoid rejecting variables that are
156 important, but which are not principal drivers of statistical variability (Monk et al.,
157 2007). The method has been widely used beyond its original applications with flow
158 discharge time series; for example to establish associations between stream
159 temperature variability and instream communities (Jackson et al., 2007; Olden and
160 Naiman, 2010; White et al., 2017), to group relevant instream geomorphic
161 parameters for hydrological and ecological models (Singh et al., 2009; Faller et al.,
162 2016) and to identify geographical properties associated with landslide susceptibility
163 (Komac, 2006). At the core of this paper is an application of this methodology to fine
164 sediment ingress. It is motivated by a conviction that the design and implementation
165 of strategies that aim to manage levels of fine sediment storage in rivers would
166 benefit from a better understanding of how facets of flow and sediment regimes
167 relate to ingress rates.

168 This paper utilises novel measurements of fine sediment ingress collected over
169 several months. These data were used with time series of discharge and turbidity,
170 where the latter is shown to be representative of fine sediment availability, to identify
171 key drivers of sediment ingress using the ecohydrological 'redundancy' approach.
172 This analysis reveals the exploratory power of facets of the discharge and turbidity
173 regimes as predictors of fine sediment ingress into riverbeds and seeks to establish
174 the potential of employing simple empirical models, at temporal and spatial scales
175 relevant to catchment management, using variables that are easily collected in the
176 field.

177 A two-stage approach was employed:

- 178 i) Classification of hydrological and turbidity time series into a small subset of
179 indices that effectively characterise the dominant components (facets) of the
180 series via a principal component analysis and redundancy reduction
181 methodology (sensu Olden and Poff, 2003).
- 182 ii) Examination of the dominant facets of turbidity and discharge that influence
183 sediment ingress using correlation matrices and the development of linear
184 regression models using the principal component sample scores.

185

186 **2. Material and Methods**

187 **2.1 Study Sites**

188 Data was collected from two lowland rivers in Rutland, UK; the River Gwash (52°38'
189 N, 00°44'W) and the River Chater (52°37' N, 00° 44'W). At the sites where
190 measurements were made, the rivers are broadly comparable in physical
191 characteristics (channel size, water chemistry, altitude and geology). The two sites
192 are only 2.6 km apart geographically and therefore experienced similar synoptic
193 meteorology and hydrological regimes. Close to the catchment outlet, mean flow is
194 $0.18 \text{ m}^3 \text{ s}^{-1}$ and Q_{10} (90th percentile) flow is $0.449 \text{ m}^3 \text{ s}^{-1}$ for the River Chater. For the
195 river Gwash mean flow is $0.52 \text{ m}^3 \text{ s}^{-1}$ and Q_{10} flow is $1.16 \text{ m}^3 \text{ s}^{-1}$ (NRFA, 2017).

196 Catchment geology is dominated by Jurassic mudstones and sandstones (British
197 Geological Survey, 2008) with both field sites located adjacent to arable farmland.
198 Surface and subsurface bed material consisted of mixed cobbles and gravel (Table
199 1). Invasive signal crayfish, *Pacifastacus leniusculus* (Dana), are present in high
200 abundances in the River Gwash but historic routine sampling by the Environment

201 Agency of England and Wales and contemporary sampling during the study period
202 by the author has not recorded any individuals in the River Chater. Previous work
203 has suggested that signal crayfish are significant biogeomorphic agents capable of
204 mobilising fine sediment (Harvey et al., 2014; Rice et al., 2014; 2016; Cooper et al.,
205 2016) although this was not an explicit consideration in the research reported here.

206

207 **2.2 Discharge data**

208 Hydrological variability during the sampling period was analysed using data collected
209 from local Environment Agency gauging stations on the River Chater (Fosters
210 Bridge; 52°38' N, 00° 35' W) and River Gwash (Manton; 52°38'N, 00° 42' W) at 15-
211 minute resolution. Discharge data ($\text{m}^3 \text{s}^{-1}$) were converted to hourly averages to
212 facilitate the identification of marked differences in the series including known
213 hydrological events (floods or low flows; Figure 1a). The majority of the study period
214 consisted of baseflow conditions punctuated by flashy high flow events.

215 As the gauge sites were 2.9 km and 12.4 km downstream of the field sites on the
216 River Gwash and River Chater respectively, discharge values at the gauge site were
217 scaled based on the catchment drainage area of the sample site relative to the
218 gauge location.

219

220 **2.3 Turbidity data**

221 Turbidity was monitored at a 5-minute resolution using two turbidity sensors: an
222 Eureka 2 Manta sonde fitted with a self-wiping turbidity sensor (International
223 Organisation for Standardisation (ISO) 7027; 0-3000 NTU, quoted error $\pm 1\%$) was
224 deployed at Brooke on the R. Gwash and a Seametrics, Instrumentation Northwest
225 Inc. (INW) self-wiping Turbo sensor (0-3000 NTU, quoted error $\pm 2\%$) was deployed
226 at Ridlington on the R. Chater. Both sensors were independently calibrated before
227 deployment using the same turbidity standards. They were mounted horizontally
228 0.1m above the river bed with the sensors approximately 0.3m from the left bank.
229 Recording errors during the study were intermittent. Where single measurements
230 were missing, they were interpolated using a local average of the previous and
231 subsequent record. Where sections of data were in error or missing because of
232 biofouling or data-logging problems, gaps were left in the time series. Datasets ran
233 from 18th June 2015 to 24th September 2015 (98 days) with 12.0 and 18.1 days
234 removed due to recording errors at Ridlington and Brooke, respectively (Figure 1b).

235 The continuous measurements of turbidity are used here as a surrogate of
236 suspended mineral sediment concentration (SSC), and therefore of fine sediment
237 availability for ingress. Turbidity is used as an independent variable because it is a
238 measure of fine sediment availability that is easily and more readily measured than
239 SSC, therefore representing a more widely available parameter. The use of turbidity
240 as a surrogate for SSC should, however, be undertaken recognising that turbidity
241 measurements are sensitive to the physical characteristics of suspended mineral
242 sediments (colour, size, shape) and the presence of other suspended materials,
243 including organic detritus (Bilotta and Brazier, 2008). To confirm the validity of the
244 turbidity data as a representation of SSC, 93 and 206 water samples were collected
245 from Ridlington and Brooke respectively, at baseflow through to storm flow
246 conditions. Samples were collected using an ISCO 3700 automated water sampler
247 fitted with a stage-activated trigger that drew water up from an inlet hose located
248 immediately adjacent to the turbidity sensor. Samples were filtered using Whatman
249 0.7µm glass microfiber filters and analysed for percent organic matter and carbonate
250 content through Loss-On-Ignition (LOI; Dean, 1974). The average organic
251 component of samples was high at Brooke (21.5%, SD = 5.36%) and Ridlington
252 (26.31%, SD = 7.77%) so SSC was calculated using only the mineral mass. The
253 correlation between mineral SSC values and measured turbidity was significant ($r =$
254 0.92 , $p < 0.001$) and demonstrated a strong linear fit ($R^2 = 0.86$; Figure S1). The
255 continuous records of turbidity are therefore used as pragmatic surrogates for SSC
256 and turbidity data (NTU) throughout the subsequent analysis.

257 **2.4 Fine sediment ingress**

258 At each site, sediment traps were installed that measured the mass of fine sediment
259 ingress over 14-day deployment periods. Each trap comprised a PVC cylinder
260 (diameter 65 mm, height 200 mm) perforated with twelve horizontal holes (diameter
261 6 mm) to permit both horizontal and vertical exchange of flow and fine sediments
262 (Mathers and Wood, 2016). All cylinders were filled with a prewashed gravel
263 framework collected from each of the respective sample sites, truncated to exclude
264 grains finer than 8 mm and enclosed in a net bag (7 mm aperture). Use of the local
265 gravel framework negates the potential influence that differing framework matrices
266 have on ingress rates (Petticrew et al., 2007). Cylinders were inserted into the river
267 bed by placing the PVC cylinders onto a steel pipe (35 mm diameter) that was then

268 driven into the bed sediments and subsequently moved from side to side until a
269 sufficient sized hole was formed. Cylinders were inserted flush with the sediment
270 surface to a depth of 200 mm (Figure 2). Cylinders were left in-situ for the entire
271 sampling campaign, but every 14 days the gravel netting bag was removed and
272 replaced with a bag of clean gravel, providing a constant record of sediment
273 accumulation at a 14-day resolution. At the end of each 14-day sampling period, the
274 net bag (containing the gravel clasts) was carefully lifted out and immediately placed
275 in a plastic bag to be processed in the laboratory with any loss of fine sediment being
276 minimal. Negligible fine sediment was observed diffusing into the water column
277 during extraction with fine material being held in the interstitial spaces of the gravels.
278 Sediment traps were installed from 18th June to 24th September 2015, providing a
279 record of 98 days that consisted of seven 14-day sample sets (referred to as B1 – B7
280 for the Gwash site and R1 – R7 for the Chater site).

281 Three riffle sites were examined at Brooke and two at Ridlington (only one site was
282 considered before 2nd July 2015). At each riffle, four cylinders were installed
283 providing a total of 12 replicates at Brooke and eight at Ridlington (four until 2nd July -
284 for the first three 14-day sample sets). Cylinders were evenly spaced across the riffle
285 unit (head through to tail) because fine sediment accumulation can vary as a function
286 of longitudinal hydraulic gradients (Mathers and Wood, 2016). In total, 105 and 57
287 samples were extracted from Brooke and Ridlington respectively (a total of three
288 cylinders could not be retrieved at both sites during the campaign).

289 In the laboratory, the contents of the cylinder samples were passed through 4 and 2
290 mm sieves to remove the framework substrate and left to settle in a container. Fine
291 sediment samples (< 2 mm) were oven dried at 60°C until a constant weight was
292 recorded. Samples were gently disaggregated, passed through a sieve nest (1000
293 µm and 125 µm) and each fraction weighed to determine the grain size distribution in
294 four grain size categories (total mass < 2000 µm, 1000-2000 µm, 125-1000 µm;
295 <125µm). These separate grain size fractions were examined because the rate of
296 fine sediment ingress is inherently associated with site-specific size ratios of
297 infiltrating particles to framework gravels (Frings et al., 2008). The total mass of
298 material < 2000 µm collected in each 14-day sampling period for Brooke and
299 Ridlington is shown in Figure 1c

300 **2.5 Identification of time series facets via the redundancy approach**

301 Spearman's rank correlation coefficients were calculated for hourly averaged flow
302 and turbidity time series to establish whether there was any simple association
303 between the two datasets. Preliminary analysis indicated that discharge values
304 differed by site and so prior to subsequent analysis, flow data were scaled to Z-
305 scores to enable comparison across sites. 23 turbidity and 14 flow indices (see Table
306 2 for definitions) were calculated for each 14-day sampling period at Ridlington and
307 Brooke. Indices were based on four facets of the two regimes: (i) magnitude – the
308 quantity measured at a sampling point at a given time including minimum and
309 maximum; (ii) frequency – how often the time series moved above a given
310 magnitude; (iii) duration – the period of time over a specific threshold; and (iv) rate of
311 change – how quickly the time series changes from one magnitude to another
312 (Richter et al., 1996; Poff et al., 1997). Previous applications of Richter's (1997)
313 methodology have focussed on characterising hydrological series for the purpose of
314 identifying ecohydrological associations over multiple years, so the most relevant
315 indices were adapted for the shorter timeseries used here (Richter et al., 1997;
316 Olden and Poff, 2003; Monk et al., 2007). In addition, a number of indices were
317 calculated that aimed to characterise the potential effect of biotic diurnal bioturbation
318 (by crayfish) on the turbidity series (cf Rice et al., 2014; 2016): average night
319 turbidity – AVNt; average day turbidity – AVDt; difference in day – night turbidity –
320 DDNt; and periodicity – PERt. Night was employed as a fixed time window (18:00-
321 6:00; Rice et al., 2014).

322 Both hydrological and turbidity indices were analysed using principal component
323 analysis (PCA) to identify redundant interrelated indices whilst retaining the major
324 sources of statistical variation (Jolliffe, 1986). A series of PCAs were undertaken on
325 turbidity and hydrological data in isolation and in combination using the 'prcomp'
326 function in R version 3.2.2. PCAs were conducted to identify the dominant indices
327 following the PCA redundancy reduction approach outlined by Olden and Poff
328 (2003). Previous research employing this approach has typically utilized a maximum
329 of six indices to sufficiently characterise the regimes (Monk et al., 2007; Belmar et
330 al., 2013; Worrall et al., 2014) and consequently the six indices with the highest
331 loadings on the first two principal component (PC) axes were identified for each set
332 of variables (turbidity, hydrological and combined hydrological and turbidity).

333 Following Olden and Poff (2003), the number of indices selected from each axis was
334 proportional to the variance explained by each PC relative to the others. For
335 example, based on the turbidity data, the first PC explained 48.4% of the total 68.5%
336 of the variance explained by the two significant components, resulting in four indices
337 being selected from PC1 and two from PC2. Highly correlated variables, with
338 Pearson's r values greater than 0.95, were considered redundant and removed to
339 retain six indices that effectively characterised statistical variability whilst minimising
340 collinearity (Monk et al., 2006).

341 **2.6 Relationship between turbidity, discharge and fine sediment ingress**

342 To examine the relationship between standardised discharge, turbidity and mass of
343 ingress, Spearman's rank correlation matrices were constructed for all 37 indices
344 and four ingress size categories. This enabled determination of the relative
345 association of individual components of turbidity and discharge with sediment
346 ingress. To assess the association of multiple facets of turbidity and discharge with
347 ingress, the PC components (sample axis scores) resulting from the reduced set of
348 variables in each dataset were used as independent variables to develop multiple
349 linear regression models. In these models the dependent variables were mass of
350 infiltrated sediment in each grain size fraction and the independent variables were
351 PC components (axes scores). PC components with eigenvalues >1 were
352 considered for inclusion in each model, and stepwise selection using the '*stepAIC*'
353 function in the '*MASS*' package was used to select the best combination of variables
354 (Venables and Ripley, 2002). As a result of the removal of highly correlated and
355 redundant variables through PCA selection and the subsequent
356 compartmentalisation of the data to reduce its dimensionality, overfitting of models
357 was minimal. This approach generated models using (1) discharge PC components,
358 (2) turbidity PC components or (3) discharge and turbidity PC components together,
359 to predict each of the grain size mass fractions. This enabled an evaluation of the
360 relative contribution to the explanatory power exerted by each driver (discharge or
361 turbidity) independently and combined on the mass of sediment ingress by size
362 fraction. To assess whether the turbidity or discharge regimes differed by site or time
363 as a function of any facets of the series (e.g. magnitude and duration), a Generalised
364 Linear Model (GLM) was fitted to the PC component scores using the '*glm*' function

365 in the 'stats' package with a Gaussian error distribution. All statistical tests were
366 conducted in the R environment (R Development Core Team, 2017).

367

368 **4. Results**

369 **4.1 Selection of turbidity and discharge variables**

370 When PCA was employed to determine which turbidity and hydrological indices were
371 most influential in characterising the dominant sources of variability, the percentage
372 of variance explained ranged from 87.07% for the combined variables (turbidity and
373 hydrology together) through to 98.18% for the reduced number of hydrological
374 indices (Table 3). Turbidity indices demonstrated the greatest variability compared to
375 hydrological indices, with less variance being explained on the first axis in both
376 instances for the full and reduced number of indices.

377

378 Using the PCA selection procedure for the turbidity variables, three indices were
379 identified that represented magnitude of turbidity (median, average night and
380 average difference in day and night turbidity values), two that represented the
381 duration of turbidity events (duration over 10 NTU and duration over 100 NTU) and
382 one that characterised the rate of change in turbidity (number of rises in the turbidity
383 series; Figure 3a). Within the subset of six hydrological variables identified, the
384 majority represented magnitude of discharge (minimum, average and standard
385 deviation of discharge), two characterised the duration of discharge events above or
386 below a threshold (duration under 0.1 scores, and duration over 14 day average
387 discharge) and one characterised the rate of change in the discharge regime (number
388 of rises in discharge series; Figure 3b). When both environmental factors (turbidity
389 and hydrology) were considered together, turbidity accounted for a larger proportion
390 of variance with four dominant turbidity indices and two hydrological indices
391 identified. Magnitude characteristics of the time series were the primary source of
392 variability (median discharge, standard deviation in discharge, median turbidity,
393 maximum turbidity and average turbidity) and the remaining two indices represented
394 the duration of low magnitude events (duration under -0.1 discharge scores and
395 duration under 10 NTU; Figure 3c).

396 **4.2 Turbidity and discharge regimes characterisation**

397 Examination of the sample sites on the ordination plots and via general linear
398 regression of the first two PC axes scores, indicated that both sites were similar in
399 character regardless of the presence of crayfish (Figure 3; $p > 0.05$ in both GLM
400 models). Despite this, Ridlington exhibited greater variation in turbidity over time,
401 with the majority of Brooke sites forming a cluster at the centre of the plot. Three
402 turbidity series represent extreme outliers, with Ridlington sample set one (R1) being
403 strongly associated with higher than average median turbidity, Ridlington set six (R6)
404 by average night turbidity values and duration over 100 NTU and Brooke set one
405 (B1) by difference in day and night turbidity. The dominant vectors of variation are
406 associated with the duration of events over 10 NTU and difference in day versus
407 night turbidity.

408 Discharge exhibited greater variability, with a wide spread of sites over time: the
409 majority of sites were heavily loaded on PC1, which was associated with low flow
410 conditions (Figure 3). Time periods in which baseflow conditions were dominant (e.g.
411 B2, R1, R4, B4) plot to the right of the ordination and those with high flow events plot
412 to the left (e.g. R6, R5, B3). When hydrological and turbidity variations were
413 considered in combination, sites plotted consistently together (Figure 3c). The
414 dominant vectors of variation were associated with low flow periods (duration under
415 0.1 discharge scores and standard deviation of discharge) with two outliers that were
416 strongly influenced by turbidity (median turbidity –Ridlington set one, R1 and
417 maximum turbidity – Ridlington set two, R2).

418 ***4.3 Discharge, turbidity and fine sediment ingress associations***

419 Discharge and turbidity time series (hourly averaged data) yielded weak associations
420 at both sites (Brooke $r_s = 0.040$; $p < 0.05$; Ridlington $r_s = 0.211$; $p < 0.001$). However,
421 moderate associations ($r_s > 0.5$) were apparent between some turbidity and
422 discharge indices (Table 4). 16 out of 23 discharge variables were associated with
423 the magnitude of the turbidity regime (i.e. maximum, minimum, range and standard
424 deviation of turbidity) and 11 of these associations were significant ($p < 0.05$; Table
425 4). Of the remaining correlations, four were characterised by duration (three of which
426 were significant), and two with frequency of turbidity events (both of which were
427 significant). Duration of discharge was the main facets of the regime associated with
428 turbidity events, with 14 discharge variables demonstrating moderate relations with

429 turbidity (12 of which were significant), followed by magnitude of discharge (seven
430 variables) and frequency of discharge events (two variables). The strongest
431 correlation was between the duration over the 14-day average discharge (D14AVd)
432 and the number of peaks over 100 NTU (NP100t; Table 4). Duration over the 14 day-
433 averaged discharge (D14AVd) was most strongly associated with turbidity
434 parameters.

435 In contrast, discharge and turbidity indices yielded weak associations with the mass
436 of sediment that infiltrated into traps (Table 5). Only three turbidity indices and one
437 discharge index had a moderate correlation ($r_s > 0.5$) with any of the different size
438 fractions of deposited sediment. The strongest correlation was between duration of
439 discharge over the 14-day average (D14AVd) and mass of fines in the size fraction
440 125-1000 μm ($r_s = 0.617$; $p \leq 0.05$). Grains in the size fraction 1000-2000 μm
441 displayed the strongest correlation with turbidity, with three indices having moderate
442 correlations, whilst total mass < 2000 μm was correlated with duration over 14 day
443 average discharge (D14AVd ; Table 5).

444 Linear regression models developed for mass of deposited fines using the PC scores
445 explained between 8.78% and 53.92% of the variance in the mass of ingress (Table
446 6). For grains 1000- 2000 μm , discharge was the most influential predictor with the
447 model accounting for an additional 15.96% of the variance compared to turbidity
448 alone or 9.56% for turbidity and hydrology combined. The duration and magnitude of
449 high flow events were the most significant predictor variables ($p = 0.004$; Table 7).

450 The mass of sediment deposited in the range 125-1000 μm was strongly influenced
451 by turbidity with the model accounting for 45% of variation, 10% greater than for
452 discharge (Table 6). Both principal components were significant predictors with the
453 duration and magnitude of turbidity values being the dominant explanatory factors
454 (Table 7). The combination of discharge and turbidity parameters only accounted for
455 an additional 0.9% of variation and the final model developed using PC components
456 only characterised the turbidity series using PC1 and PC3 scores (Tables 6 & 7).

457 For grains <125 μm , mass of deposition was predominantly explained by turbidity,
458 with the model accounting for 53.52% of variation, 32.42% more than the discharge
459 model (Table 6). PC2 was the most significant predictor ($p = 0.005$) which

460 characterised the magnitude of the turbidity regime (average conditions) and
461 duration of low turbidity events. When total mass (<2000 μm) was considered,
462 turbidity was the most influential factor (37.15%) and the magnitude and frequency of
463 high turbidity events were the dominant predictors ($p = 0.047$; Tables 6 & 7).
464 Similarly, the combined model (hydrological and turbidity) provided the best fit and
465 PC components that characterised the average, maximum and duration of low
466 turbidity elements of the regime were significant (Table 6). A summary of the multiple
467 linear regression models and the interpretations of the PC loadings for each of the
468 compartments are provided in Tables 6 and 7.

469 **5. Discussion**

470 This study investigated whether facets of discharge and turbidity time series can be
471 used to predict fine sediment ingress measured at multiple locations over several
472 months. It adopted a technique from ecohydrology, not previously applied to this
473 problem and uses robust and widely applicable parameters that can be readily
474 measured in the field. Discharge and turbidity have a relatively weak relationship
475 with each other and with mass of fine sediment ingress when individual facets of the
476 time series (e.g. magnitude or duration indices) are considered in isolation. In
477 contrast, the application of a well-established 'redundancy approach' and principal
478 component analysis enabled the fitting of multiple linear regression models, using
479 combinations of time series facets, that accounted for a larger proportion of variation
480 in the mass of fine sediment ingress. Turbidity, as a surrogate for suspended
481 sediment availability, exerted a greater influence than discharge. These results
482 indicate the potential of this method to be a useful tool for developing predictive
483 models of fine sediment ingress at scales that are relevant to sediment
484 management. Further testing and validation is required to evaluate the method's
485 applicability across different river types, flow and sediment regimes.

486

487 ***5.1 The relative role of discharge and turbidity in controlling fine sediment*** 488 ***ingress***

489 When the individual regime facets (i.e. magnitude, duration, frequency) of turbidity
490 and discharge time series were considered, there were no significant associations
491 with the mass of infiltrated sediment. This indicates that, in isolation, individual flow
492 or sediment availability parameters are likely to be weak predictors of sediment

493 ingress. The lack of apparent correlation between suspended sediment availability
494 and discharge also indicates that processes other than hydrological drivers may
495 affect changes in turbidity concentrations, including, for example, biotic processes
496 (Rice et al., 2012; Atkinson et al., 2017). Whatever the cause, temporal variations in
497 suspended sediment transport are important and are driven independently of
498 discharge.

499

500 In contrast, the application of linear regression using multiple facets of the discharge
501 and turbidity regimes yielded improved associations, indicating that it is not a single
502 element of discharge or turbidity that controls ingress, but a combination of multiple
503 facets. This also clearly highlights the advantages of employing principal component
504 analysis to distil time series datasets into a manageable number of unrelated
505 variables and so avoid overfitting models. The construction of linear regression
506 models using PC sample axis scores indicated that turbidity variables explained a
507 greater proportion of the statistical variance in deposition than discharge variables.
508 This suggests that the collection of high quality, turbidity time series data should be
509 a priority in order to corroborate and develop the findings of this study, perhaps for
510 different flow conditions and different river typologies.

511

512 ***5.2 Individual grain size associations with discharge and turbidity***

513 The strongest association in this study was between the ingress of grains <125 μm
514 and turbidity, with the turbidity model accounting for 54 % of the variation (with only
515 an additional 0.4 % explained when discharge indices were incorporated). The
516 duration that turbidity was over 10 NTU was the most significant explanatory
517 variable. Grains in this size fraction, once in suspension, can be transported long
518 distances over extended time-periods because only low energy hydraulic conditions
519 are needed to entrain them and keep them in suspension (Lambert and Walling,
520 1988). Consequently, as the amount of time with turbidity levels are above 10 NTU
521 decreases, ingress of this size range may increase because fine sediment is
522 available for deposition. Discharge had the weakest association with this size
523 fraction (21 % variance explained) with rivers often acting as an effective
524 conveyance system for silt sized particles, irrespective of hydraulic energy. Grains in
525 the size fraction 125 -1000 μm were predominantly predicted by variables which

526 characterised the magnitude of turbidity, with an explanatory power of 45%, and
527 discharge indices provided little improvement (0.9 %) if incorporated.

528 The only grain size to be predominately associated with discharge was the size
529 fraction 1000-2000 μm . The duration and magnitude of high discharge, accounted for
530 25 % of the variability in ingress rates compared to 9 % and 15 % for the turbidity
531 and combined models, respectively. Grains in this size fraction are heavily reliant on
532 sufficient hydraulic stress for entrainment and suspension. Turbidity is not an
533 important driver because grains of this size are unlikely to remain in suspension and
534 be available for deposition during long baseflow periods (Rathburn and Wohl, 2003).

535 ***5.3 Principal component analysis as a tool to upscale the temporal controls on*** 536 ***fine sediment ingress***

537 A significant gap in understanding and managing fine sediment ingress into river
538 beds is the difficulty of scaling up fine-scale process understanding, partly because
539 the key drivers are highly variable in space and time. Larger scale drivers, including
540 discharge and sediment availability, vary on synoptic to annual timescales, and may
541 provide an alternative means of modelling fine sediment deposition that is especially
542 pertinent to management questions. However, investigation of relations at these
543 larger scales has been limited by an absence of time series of sediment deposition
544 and sediment availability (Gray and Gartner, 2009). Using turbidity as a surrogate for
545 sediment concentration, longer, high-resolution datasets can now be routinely
546 collected (Loperfido et al., 2010), albeit subject to appropriate local calibration and
547 evaluation (Bilotta and Brazier, 2008).

548 Turbidity time series and gauged discharge data collected over a 14-week study
549 period on two rivers were used in this study to gain a better understanding of how
550 localised and temporal variations in discharge and turbidity influence the mass of
551 sediment deposited in a clean gravel framework. The methodological approach
552 employed highlights the potential value of undertaking principal component analysis
553 to characterise the overall facets of discharge and turbidity regimes that influence
554 fine sediment ingress and which can therefore inform large scale catchment
555 sediment management practices. The approach is empirical, seeking site-specific
556 relations between ingress, discharge and sediment availability. Its application and

557 testing in additional field situations may yield wider generic understanding of
558 important controls at these scales.

559 Despite the potential utility of the approach, it is important to exercise caution when
560 employing data redundancy approaches, such as PCA, because they may reject
561 variables of importance due to the assumption that statistically dominant sources of
562 variability are the principal drivers of the association they are being used to describe
563 (Monk et al., 2007). Nevertheless, as applied here, the approach enables
564 characterisation of the key drivers of sediment ingress, improving our knowledge of
565 the time series and, by inference, processes that are relevant to sediment loading at
566 a scale appropriate for management strategies.

567 **6. Conclusion**

568 This study demonstrates, for the first time, that an adapted PCA-based data
569 redundancy reduction method (sensu Olden and Poff, 2003) can effectively be used
570 to identify the dominant facets of turbidity and discharge time series that influence
571 the mass of fine sediment ingress into gravel river beds. The results from this study
572 of two lowland rivers in England, indicate that discharge is weakly associated with
573 ingress rates and that localised turbidity variations explain a greater amount of the
574 variance in fine sediment deposition into clean gravels. In particular, the magnitude
575 facet of the turbidity regime are important for the ingress of grains in the size fraction
576 125 – 1000 μm , whilst magnitude and the duration of turbidity events below 10 NTU
577 are associated with grains in the size fraction $<125 \mu\text{m}$.

578 The study highlights the need for additional research that simultaneously monitors
579 turbidity (or sediment concentrations), discharge and ingress rates during a range of
580 flow conditions. It is widely acknowledged that discharge during extreme flow periods
581 exerts a strong control over ingress rates (Frostick et al., 1984), but much less is
582 known about deposition rates and the principal drivers of this process during
583 baseflow conditions. Further understanding could be obtained by monitoring the
584 gradients of vertical and lateral hydrological exchange as a function of discharge, as
585 these exchanges exert a significant influence over ingress rates during baseflow
586 (Pettricrew et al., 2007).

587

588 **Acknowledgements**

589 KLM acknowledges the support of a Glendonbrook doctoral studentship and co-
590 funding from the Environment Agency to undertake this study. Thanks go to Matthew
591 Hill and James Smith who provided assistance with the fieldwork collection, Richard
592 Harland for providing technical and laboratory support and Samuel Dixon for help in
593 the collection of substrate for the sediment traps. The authors thank the comments of
594 two anonymous reviewers and the editor that have helped improved the clarity of the
595 study.

596

597 **References**

598 Abdi, H., Williams, L.J., 2010. Principal component analysis. Wiley interdisciplinary
599 reviews: computational statistics 2, 433-459. doi:10.1002/wics.101.

600 Acreman, M.C., Ferguson, A.J.D., 2010. Environmental flows and the European
601 water framework directive. *Freshwater Biol.* 55, 32-48. doi: 10.1111/j.1365-
602 2427.2009.02181.

603 Albertson, L.K., Allen, D.C., 2015. Meta-analysis: abundance, behavior, and
604 hydraulic energy shape biotic effects on sediment transport in streams. *Ecology* 96,
605 1329-1339. doi: 10.1890/13-2138.

606 Arthington, A.H., Bunn, S.E., Poff, N.L., Naiman, R.J., 2006. The challenge of
607 providing environmental flow rules to sustain river ecosystems. *Ecol. Appl.* 16, 1311-
608 1318. doi: 10.1890/1051-0761(2006)016[1311:TCOPEF]2.0.CO;2.

609 Atkinson, C.L., Allen, D.C., Davis, L., Nickerson, Z.L., 2017. Incorporating
610 ecogeomorphic feedbacks to better understand resiliency in streams: A review and
611 directions forward. *Geomorphology* DOI: 10.1016/j.geomorph.2017.07.016.

612 Belmar, O., Velasco, J., Gutiérrez-Cánovas, C., Mellado-Díaz, A., Millán, A., Wood,
613 P.J., 2013. The influence of natural flow regimes on macroinvertebrate assemblages
614 in a semiarid Mediterranean basin. *Ecohydrology* 6, 363-379. doi:
615 10.1002/eco.1274 .

616 Beschta, R.L., Jackson, W.L., 1979. The intrusion of fine sediments into a stable
617 gravel bed. *Journal of the Fisheries Board of Canada* 36, 204-210. doi:
618 bs/10.1139/f79-030#.WT6DF8uGOUk.

619 Beschta, R.L., Jackson, W.L., Knoop, K.D., 1981. Sediment transport during a
620 controlled reservoir release. *Water Resour Bull.* 17, 635-641. doi: 10.1111/j.1752-
621 1688.1981.tb01270.x.

622 Bilotta, G.S., Brazier, R.E., 2008. Understanding the influence of suspended solids on
623 water quality and aquatic biota. *Water Res.* 42, 2849-2861. doi:
624 10.1016/j.watres.2008.03.018.

625 British Geological Survey, 2008. Digital Geological Map Data of Great Britain - 625k

- 626 (DiGMapGB-625) Dykes version 5.
- 627 Brunke, M., 1999. Colmation and depth filtration within streambeds: retention of
628 particles in hyporheic interstices. *International Review of Hydrobiology*, 84, 99-117.
629 doi/abs/10.1002/iroh.199900014
- 630 Buffington, J.M., Montgomery, D.R., 1999. Effects of hydraulic roughness on surface
631 textures of gravel-bed rivers. *Water Resour. Res.* 35, 3507-3521. doi:
632 10.1029/1999WR900138.
- 633 Carling, P.A., 1984. Deposition of fine and coarse sand in an open-work gravel bed.
634 *Can. J. Fish. Aquat. Sci.* 41, 263-270. doi: abs/10.1139/f84-030#.WT6Eb8uGOUk.
- 635 Carling, P.A., McCahon, C.P., 1987. Natural siltation of brown trout (*Salmo trutta* L.)
636 spawning gravels during low-flow conditions. In Craig, J.F. and Kemper, B.J.
637 *Regulated streams: Advances in Ecology*. Plenum Press: New York.
- 638 Collins, A.L., Naden, P.S., Sear, D.A., Jones, J.I., Foster, I.D., Morrow, K., 2011.
639 Sediment targets for informing river catchment management: international
640 experience and prospects. *Hydrol. Process.* 25, 2112-2129. doi: 10.1002/hyp.7965.
- 641 Cooper, R.J., Outram, F.N., Hiscock, K.M., 2016. Diel turbidity cycles in a headwater
642 stream: evidence of nocturnal bioturbation?. *J. Soils Sediments*, 16, 1815-1824. doi:
643 10.1007/s11368-016-1372-y.
- 644 Dean, W. E., 1974. Determination of carbonate and organic matter in calcareous
645 sediments and sedimentary rocks by loss on ignition; comparison with other
646 methods. *Journal of Sedimentary Research* 44, 242-248.
- 647 Diplas, P., Parker, G., 1992. Deposition and removal of fines in gravel-bed streams.
648 In. Billi, P., D. Hey, C.R. Thorne and P. Tacconi. *Dynamics of gravel-bed rivers*, John
649 Wiley and Sons: Chichester.
- 650 Einstein, H.A., 1968. Deposition of suspended particles in a gravel bed. *Journal of*
651 *the Hydraulics Division*, 94, 1197-1206.
- 652 Faller, M., Harvey, G.L., Henshaw, A.J., Bertoldi, W., Bruno, M.C., England, J., 2016.
653 River bank burrowing by invasive crayfish: Spatial distribution, biophysical controls
654 and biogeomorphic significance. *Sci. Total Environ.* 569, 1190-1200.
- 655 Franssen, J., Lapointe, M., Magnan, P., 2014., Geomorphic controls on fine
656 sediment infiltration into salmonid spawning gravels and the implications for
657 spawning habitat rehabilitation. *Geomorphology*, 211, 11-21. doi:
658 10.1016/j.geomorph.2013.12.019.
- 659 Frings, R.M., Kleinhans, M.G., Vollmer, S., 2008. Discriminating between pore –
660 filling load and bed-structure load: a new porosity-based method, exemplified for the
661 river Rhine. *Sedimentology* 55, 1571-1593. doi: 10.1111/j.1365-3091.2008.00958.x.

- 662 Frostick, L.E., Lucas, P.M., Reid, I., 1984. The infiltration of fine matrices into coarse-
663 grained alluvial sediments and its implications for stratigraphical interpretation. *J.*
664 *Geol. Society.* 141, 955-965. doi: 10.1144/gsjgs.141.6.0955.
- 665 Gibson, S., Abraham, D., Heath, R., Schoellhamer, D., 2009. Bridging process
666 threshold for sediment infiltrating into a coarse substrate. *J. Geotech. Geoenviron.*
667 136, 402-406. doi: 10.1061/%28ASCE%29GT.1943-5606.0000219.
- 668 Gray, J.R., Gartner, J.W., 2009. Technological advances in suspended-sediment
669 surrogate monitoring. *Water Resour. Res.* 45,. Doi: 10.1029/2008WR007063.
- 670 Harvey, G.L., Henshaw, A.J., Moorhouse, T.P., Clifford, N.J., Holah, H., Grey, J.,
671 Macdonald, D.W., 2014. Invasive crayfish as drivers of fine sediment dynamics in
672 rivers: field and laboratory evidence. *Earth Surf. Processes.* 39, 259-271. Doi:
673 10.1002/esp.3486.
- 674 Heppell, C.M., Wharton, G., Cotton, J.A.C., Bass, J.A.B., Roberts, S.E., 2009.
675 Sediment storage in the shallow hyporheic of lowland vegetated river reaches.
676 *Hydrol. Process.*, 23, 2239-2251. doi: 10.1002/hyp.7283.
- 677 Jackson, H.M., Gibbins, C.N., Soulsby, C., 2007. Role of discharge and temperature
678 variation in determining invertebrate community structure in a regulated river. *River*
679 *Res. Appl.*, 23, 651-669. doi: 10.1002/rra.1006.
- 680 Jolliffe, I.T., 1986. *Principal Component Analysis*, Springer-Verlag : New York.
- 681 Jones, J.I., Collins, A.L., Naden, P.S., Sear, D.A., 2012a. The relationship between
682 fine sediment and macrophytes in rivers. *River Res. Appl.*, 28, 1006-1018. doi:
683 10.1002/rra.1486.
- 684 Jones, J.I., Murphy, J.F., Collins, A.L., Sear, d.A., Naden, P.S., Armitage, P.D.,
685 2012b. The impact of fine sediment on macro-invertebrates. *River Res. Appl.*, 28,
686 1055-1071. doi: 10.1002/rra.1516.
- 687 Jones, J.I., Duerdoth, C.P., Collins, A.L., Naden, P.S., Sear, D.A., 2014. Interactions
688 between diatoms and fine sediment. *Hydrol. Process.*, 28, 1226-1237. doi:
689 10.1002/hyp.9671.
- 690 Kemp, P., Sear, D.A., Collins, A., Naden, P. Jones, I., 2011. The impacts of fine
691 sediment on riverine fish. *Hydrol. Process.*, 25, 1800-1821. doi: 10.1002/hyp.7940.
- 692 Komac, M., 2006. A landslide susceptibility model using the analytical hierarchy
693 process method and multivariate statistics in perialpine
694 Slovenia. *Geomorphology*, 74, 17-28.
- 695 Lambert, C.P., Walling, D.E., 1988. Measurement of channel storage of suspended
696 sediment in a gravel-bed river. *Catena*, 15, 65-80. doi: 10.1016/0341-
697 8162(88)90017-3.

- 698 Lapointe, M.F., Bergeron, N.E., Bérubé, F., Pouliot, M.A., Johnston, P., 2004.
699 Interactive effects of substrate sand and silt contents, redd-scale hydraulic gradients,
700 and interstitial velocities on egg-to-emergence survival of Atlantic salmon (*Salmo*
701 *salar*). *Can. J. Fish. Aquat. Sci.*, 61, 2271-2277. doi: 10.1139/f04-236.
- 702 Loperfido, J.V., Just, C.L., Papanicolaou, A.N., Schnoor, J.L. 2010. In situ sensing to
703 understand diel turbidity cycles, suspended solids, and nutrient transport in Clear
704 Creek, Iowa. *Water Resour. Res.* 46. doi: 10.1029/2009WR008293.
- 705 Mathers, K.L., Wood, P.J., 2016. Fine sediment deposition and interstitial flow effects
706 on macroinvertebrate community composition within riffle heads and tails.
707 *Hydrobiologia*, 776, 147–160. doi: 10.1007/s10750-016-2748-0.
- 708 McNeil, W.J., Ahnell, W.H., 1964. Success of pink salmon spawning relative to size
709 of spawning bed materials (No. 157). US Department of Interior, Fish and Wildlife
710 Service.
- 711 Monk, W.A., Wood, P.J., Hannah, D.M., Wilson, D.A., 2007. Selection of river flow
712 indices for the assessment of hydroecological change. *River Res. Appl.* 23 , 113-
713 122. doi: 10.1002/rra.964.
- 714 Monk, W.A., Wood, P.J., Hannah, D.M., Wilson, D.A., Extence, C.A., Chadd, R.P.,
715 2006. Flow variability and macroinvertebrate community response within riverine
716 systems. *River Res. Appl.* 22, 595-615. doi: 10.1002/rra.933.
- 717 Mustonen, K.R., Mykrä, H., Marttila, H., Haghghi, A.T., Kløve, B., Aroviita, J.,
718 Veijalainen, N., Sippel, K., Muotka, T., 2016. Defining the natural flow regimes of
719 boreal rivers: relationship with benthic macroinvertebrate communities. *Freshwater*
720 *Sci.* 35, 559-572. doi: 10.1086/685104.
- 721 Naden, P.S., Murphy, J.F., Old, G.H., Newman, J., Scarlett, P., Harman, M.,
722 Duerdoth, C.P., Hawczak, A., Pretty, J.L., Arnold, A., Laizé, C., 2016. Understanding
723 the controls on deposited fine sediment in the streams of agricultural catchments.
724 *Sci. Total Environ.* 547, 366-381. doi: 10.1016/j.scitotenv.2015.12.079.
- 725 National River Flow Archive, 2017. Available at: <https://nrfa.ceh.ac.uk/> [Access Date:
726 15 Dec 2017].
- 727 Olden, J.D., Naiman, R.J., 2010. Incorporating thermal regimes into environmental
728 flows assessments: modifying dam operations to restore freshwater ecosystem
729 integrity. *Freshwater Biol.* 55, 86-107. doi: 10.1111/j.1365-2427.2009.02179.x.
- 730 Olden, J.D., Poff, N.L., 2003. Redundancy and the choice of hydrologic indices for
731 characterizing streamflow regimes. *River Res. Appl.* 19,101-121. doi:
732 10.1002/rra.700.

- 733 Pacioglu, O., Shaw, P., Robertson, A., 2012. Patch scale response of hyporheic
734 invertebrates to fine sediment removal in two chalk rivers. *Fund. Appl. Limnology* 18,
735 283–288. doi: 10.1127/1863-9135/2012/0388.
- 736 Petticrew, E. L., Krein, A., Walling, D.E., 2007. Evaluating fine sediment mobilization
737 and storage in a gravel-bed river using controlled reservoir releases. *Hydrol.*
738 *Process.* 21, 198-210. doi: 10.1002/hyp.6183.
- 739 Petts, G.E., 1984. Sedimentation within a regulated river. *Earth Surf, Proc. Land.* 9,
740 125-134. doi: 10.1002/esp.3290090204.
- 741 Petts, G.E., 1988. Accumulation of fine sediment within substrate gravels along two
742 regulated rivers, UK. *Regul. River.* 2, 141-153. doi: 10.1002/rrr.3450020208.
- 743 Poff, N., 1996. A hydrogeography of unregulated streams in the United States and
744 an examination of scale-dependence in some hydrological descriptors. *Freshwater*
745 *Biol.* 36, 71-79. doi: 10.1046/j.1365-2427.1996.00073.x.
- 746 Poff, N.L., Allan, J.D., Bain, M.B., Karr, J.R., Prestegard, K.L., Richter, B.D.,
747 Sparks, R.E., Stromberg, J.C., 1997. The natural flow regime. *BioScience*, 47, 769-
748 784.
- 749 Poff, N.L., Zimmerman, J.K., 2010. Ecological responses to altered flow regimes: a
750 literature review to inform the science and management of environmental flows.
751 *Freshwater Biol.* 55, 194-205. doi: 10.1111/j.1365-2427.2009.02272.x.
- 752 R Core Team (2017) R: A language and environment for statistical computing. R
753 foundation for statistical computing, Vienna, Austria. URL: <http://www.R-project.org/>.
- 754 Rathburn, S., Wohl, E., 2003. Predicting fine sediment dynamics along a pool-riffle
755 mountain channel. *Geomorphology* 55, 111-124. doi: 10.1016/S0169-
756 555X(03)00135-1.
- 757 Relyea, C.D., Minshall, G.W., Danehy, R.J., 2012. Development and validation of an
758 aquatic fine sediment biotic index. *Environ. Manage.* 49, 242-252. doi:
759 10.1007/s00267-011-9784-3.
- 760 Rice, S. P., Johnson, M.F., Reid, I., 2012. Animals and the geomorphology of gravel-
761 bed rivers. In Church, M., Biron, P.M., Roy, A.J., (Eds) *Gravel-bed Rivers:*
762 *Processes, Tools, Environments*, John Wiley & Sons: Chichester.
- 763 Rice, S.P., Johnson, M.F., Extence, C., Reeds, J., Longstaff, H., 2014. Diel patterns
764 of suspended sediment flux and the zoogeomorphic agency of invasive crayfish.
765 *Cuadernos de Investigación Geográfica.* 40, 7-27.
- 766 Rice, S.P., Johnson, M.F., Mathers, K., Reeds, J., Extence, C., 2016. The
767 importance of biotic entrainment for base flow fluvial sediment transport. *J. Geophys.*
768 *Res.* 121, 890-906. doi: 10.1002/2015JF003726.

- 769 Richter, B., Baumgartner, J., Wigington, R., Braun, D., 1997. How much water does
770 a river need?. *Freshwater Biol.*, 37, 231-249. doi: 10.1046/j.1365-
771 2427.1997.00153.x.
- 772 Richter, B.D., Baumgartner, J.V., Powell, J., Braun, D.P., 1996. A method for
773 assessing hydrologic alteration within ecosystems. *Conserv. Biol.* 10, 1163-1174.
774 doi: 10.1046/j.1523-1739.1996.10041163.x.
- 775 Sear, D.A., 1993. Fine sediment infiltration into gravel spawning beds within a
776 regulated river experiencing floods: ecological implications for salmonids. *Regul.*
777 *River.*, 8, 373-390. doi: 10.1002/rrr.3450080407.
- 778 Singh, P.K., Kumar, V., Purohit, R.C., Kothari, M., Dashora, P.K., 2009. Application
779 of principal component analysis in grouping geomorphic parameters for hydrologic
780 modelling. *Water Resour. Man.* 23, 325-339.
- 781 Statzner, B., 2012. Geomorphological implications of engineering bed sediments by
782 lotic animals. *Geomorphology* 157-158, 49-65. doi:10.1016/j.geomorph.2011.03.022.
- 783 Venables, W. N., Ripley, B. D., 2002. *Modern Applied Statistics with S*. Fourth
784 Edition. Springer, New York. ISBN 0-387-95457-0
- 785 Walling, D.E., Fang, D., 2003. Recent trends in the suspended sediment loads of the
786 world's rivers. *Global Planet. Change* 39, 111-126. doi: 10.1016/S0921-
787 8181(03)00020-1.
- 788 Wharfe, D. M., Hardie, S.A., Uytendaal, A.R., Bobbi, C.J., Barmuta, L.A., 2014. The
789 ecology of rivers with contrasting flow regimes: identifying indicators for setting
790 environmental flows. *Freshwater Biol.* 59, 2064-2080. doi: 10.1111/fwb.124.
- 791 White, J. C., Hannah, D.M., House, A., Beatson, S.J.V., Martin, A., Wood, P.J.,
792 2017. Macroinvertebrate responses to flow and stream temperature variability across
793 regulated and non-regulated rivers. *Ecohydrology* 10, e1773. doi: 10.1002/eco.1773.
- 794 Wohl, E., Bledsoe, B.P., Jacobson, R.B., Poff, N.L., Rathburn, S.L., Walters, D.M.,
795 Wilcox, A.C., 2015. The natural sediment regime in rivers: broadening the foundation
796 for ecosystem management. *BioScience* 65, 358-371. doi: 10.1093/biosci/biv002.
- 797 Wolman, M.G., 1954. A method of sampling coarse river-bed material. *EOS*,
798 *Transactions American Geophysical Union* 35, 951-956. doi:
799 10.1029/TR035i006p00951
- 800 Wood, P.J., Armitage, P.D., 1999. Sediment deposition in a small lowland stream—
801 management implications. *Regul. River.*, 15, 199-210. doi: 10.1002/(SICI)1099-
802 1646(199901/06)15:1/3<199::AID-RRR531>3.0.CO;2-0.
- 803 Worrall, T.P., Dunbar, M.J., Extence, C.A., Laize, C.L., Monk, W.A., Wood, P.J.,
804 2014. The identification of hydrological indices for the characterization of

805 macroinvertebrate community response to flow regime variability. *Hydrolog. Sci. J.*,
806 59, 645-658.

807

808

809

810

811

812

813

814

815

816

817

818

819

820

821

822

823

824

825

826

827

828

829

830

831

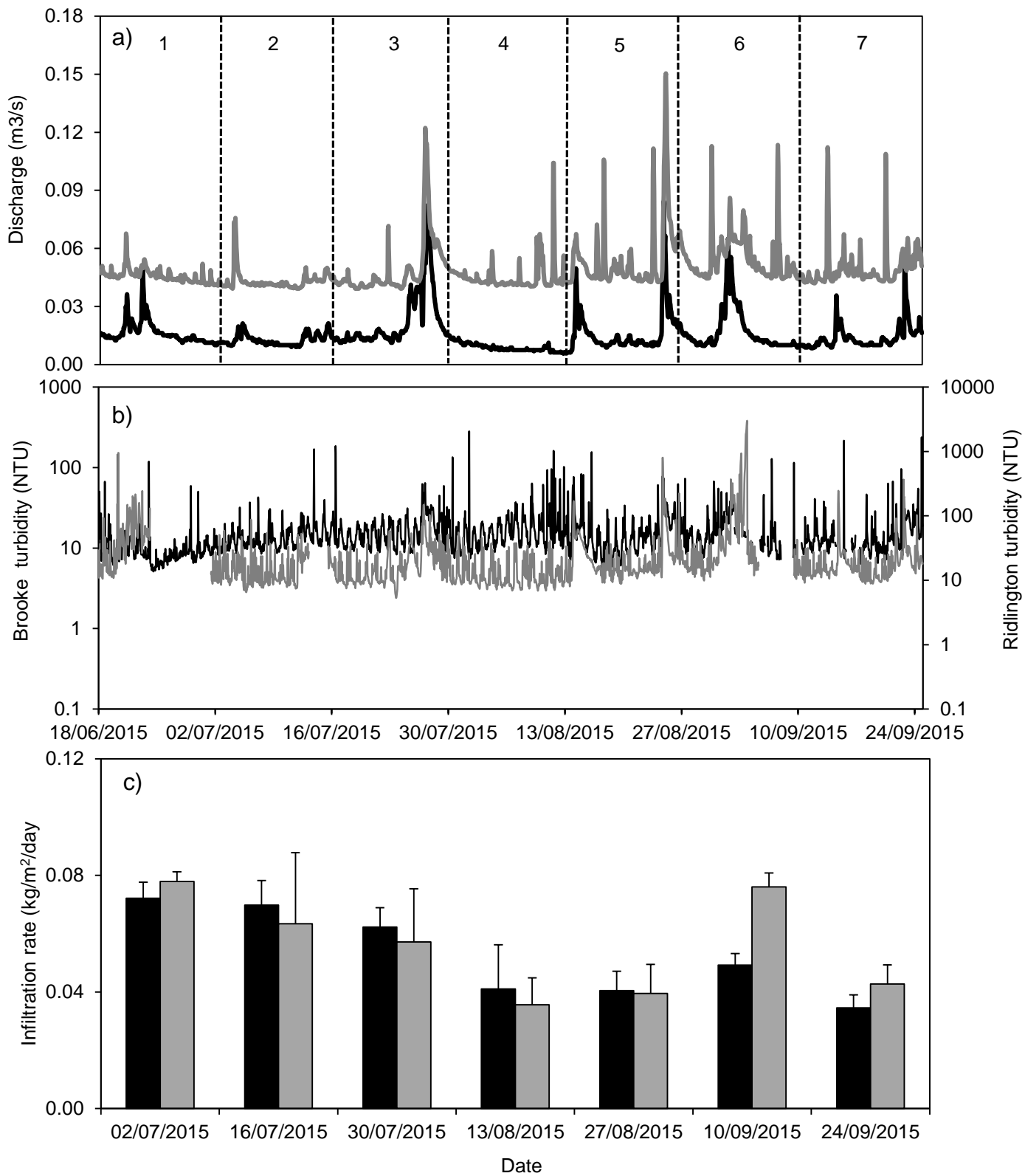


Figure 1.

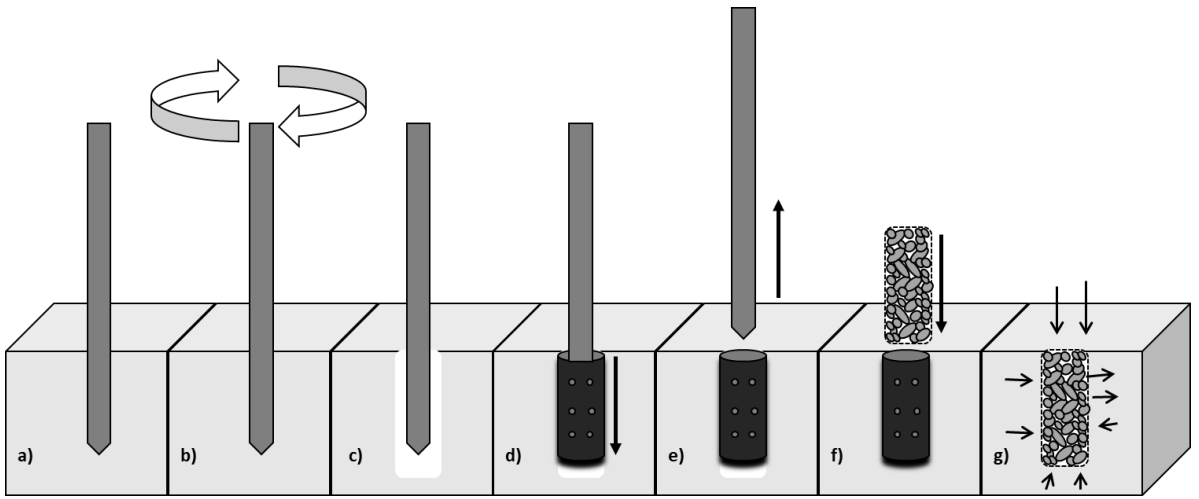


Figure 2.

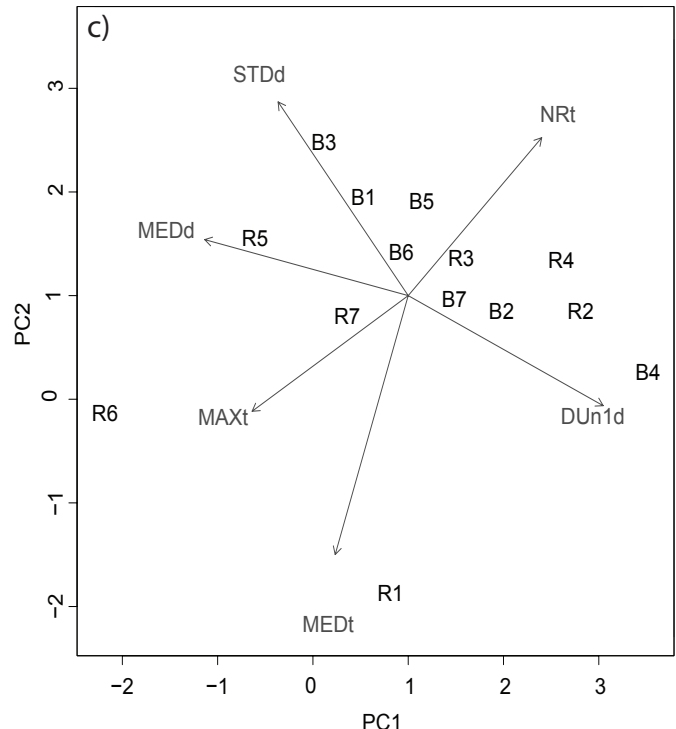
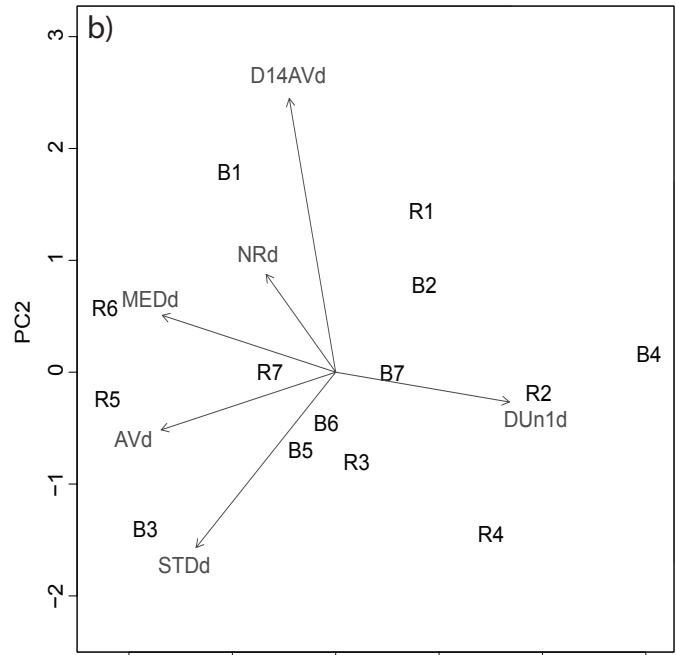
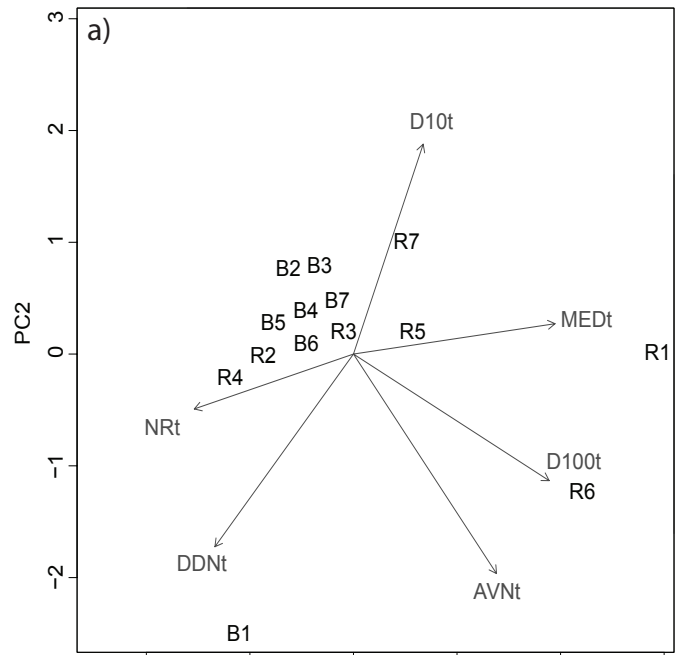


Table 1. Metrics of bed material grain size distributions, including fine sediment measures, for the study reaches

Grain size characteristic	Brooke	Ridlington
Surface ^a		
D ₁₆ (mm)	4.2	6.0
D ₅₀ (mm)	13.4	32.0
D ₈₄ (mm)	20.6	64.0
Mass < 4mm (%)	4.3	3.9
Subsurface ^b		
D ₁₆ (mm)	1.4	0.8
D ₅₀ (mm)	9.1	7.8
D ₈₄ (mm)	24.2	36.3
Mass < 2mm (%)	20.0	28.8

^a based on 400 pebble count, 200 at two riffles per site (Wolman, 1954)

^b based on four pooled McNeil samples from two riffles at each site, average sample weight 20.01 kg (McNeil and Ahnell, 1964)

Table 2. Summary of turbidity and flow indices calculated in this study.

Facet of the turbidity regime	Turbidity indices	Description	Facet of the discharge regime	Discharge indices	Description
Magnitude	MAXt	Maximum turbidity	Magnitude	MAXd	Maximum discharge
Magnitude	MINt	Minimum turbidity	Magnitude	MINd	Minimum discharge
Magnitude	RANt	Turbidity range	Magnitude	RANd	Discharge range
Magnitude	STDt	Standard deviation of turbidity	Magnitude	STDd	Standard deviation of discharge
Magnitude	AVt	14 day average turbidity value	Magnitude	AVd	14 day average discharge
Magnitude	MEDt	Median turbidity value	Magnitude	MEDd	Median discharge
Duration	D10t	Duration over 10 NTU	Duration	D1d	Duration over 0.1 (z standardised score)
Duration	D20t	Duration over 20 NTU	Duration	D2d	Duration over 0.2 (z standardised score)
Duration	D50t	Duration over 50 NTU	Duration	DUn1d	Duration under - 0.1 (z standardised score)
Duration	D100t	Duration over 100 NTU	Duration	DUn2d	Duration over - 0.2 (z standardised score)
Duration	DU10t	Duration under 10 NTU	Duration	D14AVd	Duration over 14 day average discharge
Duration	D14AVt	Duration over 14 day average turbidity value	Duration	DTAVd	Duration over total average discharge
Duration	DTAVt	Duration over total average turbidity value	Frequency	NPTAVd	Number of peaks over total average discharge
Rate of change	PERt	Periodicity	Rate of change	NRd	Number of rises in discharge series
Magnitude	AVNt	Average night turbidity value			
Magnitude	AVDt	Average day turbidity value			
Magnitude	DDNt	Average difference in day and night turbidity			
Frequency	NP20t	Number of peaks over 20 NTU			
Frequency	NP50t	Number of peaks over 50 NTU			
Frequency	NP100t	Number of peaks over 100 NTU			
Rate of change	NRT	Number of rises in turbidity series			

Table 3. Summary of the percentage variability explained on axes 1-4 for each of the six sets of variables

	Principal component (% variance explained)				Total (%)
	1	2	3	4	
All turbidity	48.39	20.06	11.47	7.15	87.07
Reduced turbidity	52.48	25.59	11.84	8.74	98.65
All hydrological	66.68	15.5	11.45	4.04	97.67
Reduced hydrological	55.41	19.87	16.30	6.60	98.18
Turbidity and hydrological combined	39.08	21.23	13.06	8.51	81.88
Reduced turbidity and hydrological	48.19	27.37	16.93	4.9	97.39

Table 4 .Spearman's rank correlations for all discharge (standardised) and turbidity indices (only those with a moderate correlation stronger than $r_s > 0.5$ are presented).

Discharge index	Turbidity index	p value
MINd	MAXt	0.546 *
MINd	RANt	0.546 *
MEDd	MAXt	0.596 *
MEDd	RANt	0.596 *
MEDd	AVt	0.595 *
MEDd	D100t	0.519
MEDd	STDt	0.522
NPTAVd	MINt	0.504
NPTAVd	NRt	-0.613
D14AVd	MAXt	0.709 ***
D14AVd	RANt	0.709 ***
D14AVd	AVt	0.630 *
D14AVd	D50t	0.570 **
D14AVd	D100t	0.720 *
D14AVd	AVNt	0.522
D14AVd	NP50t	0.541 *
D14AVd	NP100t	0.782 ***
D14AVd	STDt	0.674 *
D14AVd	D14AVt	-0.617 *
DUn1d	MAXt	-0.525
DUN2d	MAXt	-0.560 *
DUN2d	RANt	-0.560 *
DTAVd	AVt	0.530

* $p \leq 0.05$, ** $P \leq 0.01$, *** $p \leq 0.005$

Table 5. Spearman's rank correlations for discharge (standardised) and turbidity indices and ingress grain size characteristics (g; only those with a moderate correlation stronger than $r_s > 0.5$ are presented).

Grain size	Index	ρ value
Total mass < 2000 μm	D14AVd	0.566 *
1000 - 2000 μm	NP100t	0.592 *
1000 - 2000 μm	AVNt	0.560 *
1000 - 2000 μm	D100t	0.531
1000 - 2000 μm	D14AVd	0.617 *

* $p \leq 0.05$, ** $P \leq 0.01$, *** $p \leq 0.005$

Table 6. Summary of multiple linear regression models fitted to ingress rates using PC scores from turbidity, discharge and turbidity + discharge datasets (reduced). * $p \leq 0.05$, ** $P \leq 0.01$, *** $p \leq 0.005$.

Datasets	Predictor	Adjusted R²	F	Model p value	Variable p value	
Total mass <2000 μm						
Turbidity	PC1 + PC2	37.15	4.48	0.03 *	PC1 0.047	PC2 0.053
Discharge	PC2	30.03	6.58	0.03 *		
Turbidity + Discharge	PC1 + PC3	32.39	4.11	0.05 *	PC1 0.0394	PC3 0.125
1000- 2000 μm						
Turbidity	PC1	8.78	2.25	0.16		
Discharge	PC2	24.74	5.27	0.04 *		
Turbidity + Discharge	PC2	15.18	3.33	0.15		
125 – 1000 μm						
Turbidity	PC1 + PC2	45.00	6.31	0.02 *	PC1 0.020	PC2 0.043
Discharge	PC1 + PC2	35.00	4.58	0.03 *	PC1 0.106	PC2 0.032
Turbidity + Discharge	PC1 + PC3	45.90	6.52	0.01 *	PC1 0.107	PC3 0.150
<125μm						
Turbidity	PC1 + PC2	53.52	8.49	0.01 *	PC1 0.056	PC2 0.005
Discharge	PC2	20.90	4.43	0.06		
Turbidity + Discharge	PC1 + PC3	53.92	8.61	0.01 *	PC1 0.020	PC3 0.010

Table 7. Principal component loadings for the variables within the principle components analysis.

Dataset	PC1		PC2		PC3	
	Variable loadings	Interpretation	Variable loadings	Interpretation	Variable loadings	Interpretation
Turbidity	MEDt (0.52), D100t (0.51), NRt (-0.41)	Magnitude, duration and frequency of turbidity events (high)	D10t (0.56), AVNt (-0.50), DDNt (-0.51)	Duration of low turbidity events and absolute value of average turbidity conditions		
Discharge	MEDd (-0.47), DUn1d (0.47), AVd (-0.47)	Duration of low discharge events and average discharge	D14AVd (0.71), STDd (-0.55), NRd (0.33)	Duration above average discharge conditions and magnitude of discharge		
Turbidity & discharge	AVt (-0.55), MAXt (-0.51)	Average and extreme turbidity conditions	STDd (0.62), DUn1d (-0.57), MEDt (-0.44)	Magnitude of discharge and turbidity, duration of low discharge conditions	DU10t (-0.66)	Duration under low turbidity threshold

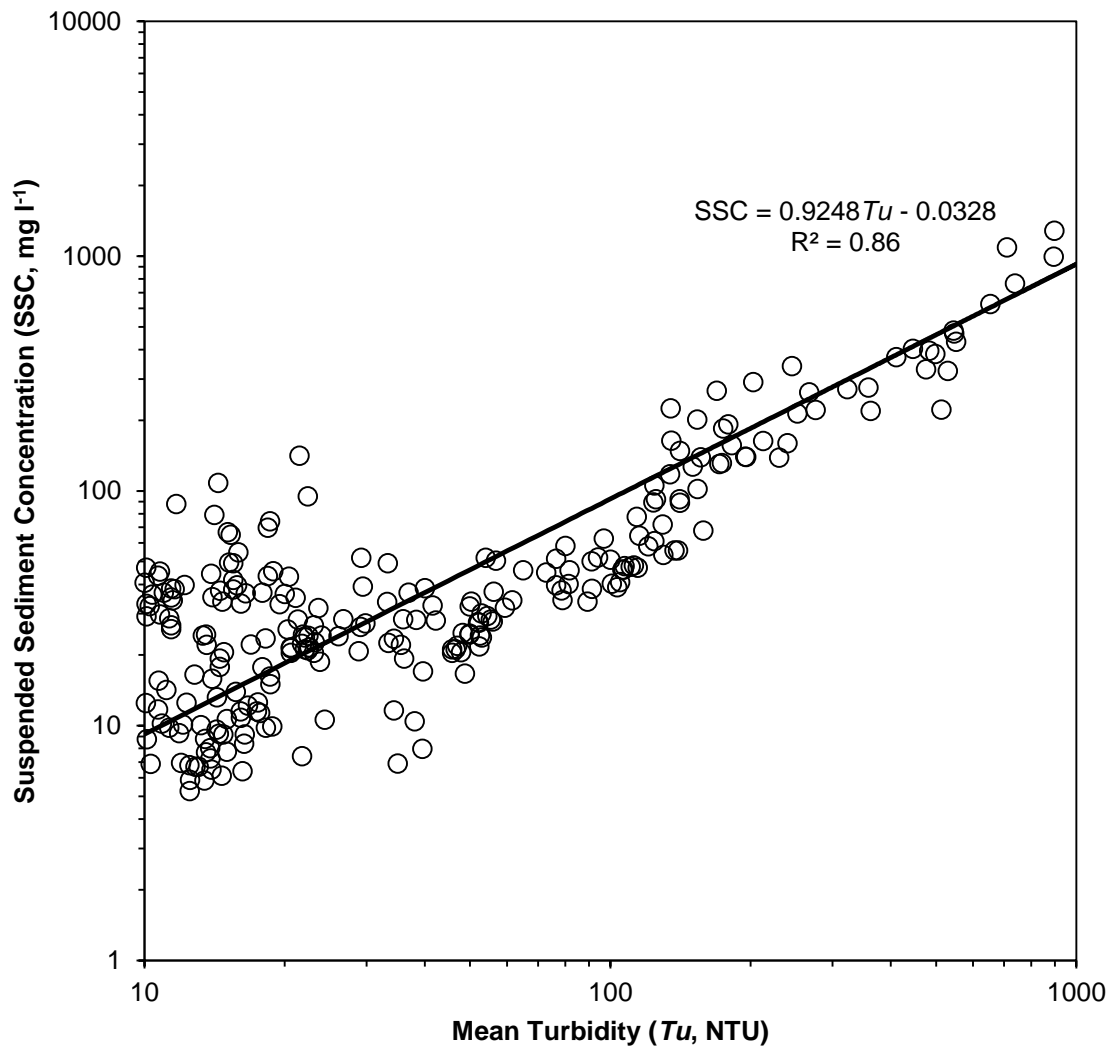


Figure S1. Relation between measure turbidity and concurrently suspended sediment concentrations from Brooke and Ridlington field sites (n = 299).